JOURNAL OF SPACECRAFT AND ROCKETS
Vol. 43, No. 2, March–April 2006

Ground-to-Space Effective Atomic Oxygen Fluence Correlation for DC 93-500 Silicone

Kim K. de Groh* and Bruce A. Banks†
NASA John H. Glenn Research Center at Lewis Field, Cleveland, Ohio 44233
and
David Ma‡
Lockheed Martin Space Systems, Sunnyvale, California 94089

The objective of this research was to calibrate the ground-to-space effective atomic oxygen fluence for DC 93-500 silicone in a thermal energy electron cyclotron resonance (ECR) oxygen plasma facility. A technique has been developed at NASA Glenn Research Center to determine the equivalent amount of atomic oxygen exposure in an ECR ground-test facility to produce the same degree of atomic oxygen damage as in space. The approach used was to compare changes in the surface hardness of ground test (ECR)-exposed DC 93-500 silicone with DC 93-500 exposed to low Earth orbit (LEO) atomic oxygen as part of a shuttle flight experiment. The ground-to-space effective atomic oxygen fluence correlation was determined based on the fluence in the ECR source that produced the same hardness for the fluence in space. A nanomechanical measurement system operated in conjunction with an atomic force microscope (AFM) was used to determine the surface hardness of the silicones. Hardness vs contact depth measurements were obtained for five ECR-exposed DC 93-500 samples (ECR exposed for 18 to 40 h, corresponding to Kapton effective fluences of 4.2×10^{20} to 9.4×10^{20} atoms/cm^2, respectively) and for space-exposed DC 93-500 from the Evaluation of Oxygen Interactions with Materials III (EOIM III) shuttle flight experiment, exposed to LEO atomic oxygen (2.3×10^{20}atoms/cm^2). Pristine controls for the ECR tests and for the EOIM III flight sample were also evaluated. A ground-to-space correlation value was determined based on correlation values for four contact depths (150, 200, 250, and 300 nm), which represent the near-surface depth data. The results indicate that the Kapton effective atomic oxygen fluence in the ECR facility needs to be 2.64 times higher than in LEO to replicate equivalent exposure damage in the ground test silicone as occurred in the space exposed silicone.

Nomenclature

A	=	area of indentation, also contact area
F	=	area function for indenter tip
H	=	hardness
h_c	=	contact depth
$h_{\max}$	=	maximum depth
P	=	load
$P_{\max}$	=	peak indentation load
S	=	gradient of the initial unloading curve
ε	=	tip geometry factor

I. Introduction

SILICONES, a family of commonly used spacecraft materials, do not chemically erode away with atomic oxygen (AO) attack like other organic materials that have volatile oxidation products. Silicones react with AO and form an oxidized hardened silicate surface layer. Often loss of methyl groups causes shrinkage of the surface skin and "mud-tile" crazing degradation. But silicones often do not lose mass,[1] and some silicones actually gain mass during AO exposure. Therefore, the effective AO fluence for silicones in a ground-test facility should not be determined based on mass loss measurements, as they typically are with polymers such as Kapton.[2] Another method for determining effective fluence needs to be used.

A technique based on changes in surface hardness has been developed at NASA Glenn Research Center at Lewis Field. Specifically, this technique has been used to determine the equivalent amount of atomic oxygen oxidation via oxide hardness measurement. The approach was to compare changes in the surface hardness of ground-laboratory-exposed DC 93-500 silicone with DC 93-500 exposed to low Earth orbit (LEO) AO as part of a shuttle flight experiment. The ground-to-space effective AO fluence was determined based on the Kapton effective fluence in the ground-laboratory facility that produced the same hardness for the fluence in space. Because microhardness measurements needed to be obtained on the very surface layer of a rubber substrate (with primarily elastic deformation), traditional techniques for microhardness characterization that apply relatively large forces and characterize hardness based on plastic deformation could not be used. Therefore, nanomechanical testing using ultra-light-load indentations and continuous load-displacement monitoring was used to determine the surface hardness of the silicones. Hardness vs contact depth were obtained for five DC 93-500 samples exposed to AO in an electron cyclotron resonance (ECR) thermal energy source facility and for space-exposed DC 93-500 from the Evaluation of Oxygen Interactions with Materials III (EOIM III) shuttle flight experiment. Ground-to-space correlation values were determined based on the near-surface depth data.

II. Experimental Procedures

A. Materials

1. DC 93-500 Silicone

The product name for DC 93-500 is Dow Corning® 93-500 Space Grade Encapsulant. It is supplied as a two-part liquid component kit. When the liquid components are thoroughly mixed, the mixture cures to a clear, flexible, low-volatility space-grade elastomer, which is suited for the protection of electrical/electronic assemblies, and has numerous other spacecraft applications. The service temperature range of DC 93-500 is −45 to +200°C (−49 to +392°F).

Received 7 December 2004; revision received 16 March 2005; accepted for publication 25 August 2005.

*Senior Materials Research Engineer, M.S. 309-2, Electro-Physics Branch, 21000 Brookpark Road.
†Chief, Electro-Physics Branch, M.S. 309-2, Electro-Physics Branch, 21000 Brookpark Road.
‡Senior Staff Engineer, M/S 7LRS/B157, Materials and Processes Engineering, 1111 Lockheed Martin Way.

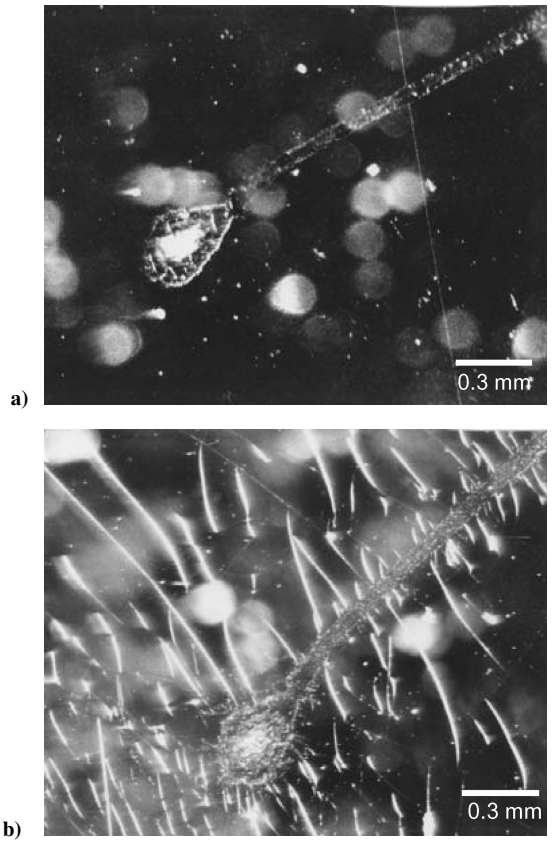

Fig. 1 Images of the EOIM III DC 93-500 sample: a) preflight and b) postflight showing surface crazing due to AO oxidation.

2. Ground-Laboratory ECR AO Exposed DC 93-500

The ground-laboratory test samples were exposed to AO in an ECR facility. These samples were approximately 0.25×0.25 in. (0.635×0.635 cm) in size, and approximately 0.020–0.025 in. (0.051–0.064 cm) thick. These samples were made to have the same thickness as the space-flight sample, as thickness variations of soft materials could affect hardness values. All samples (pristine controls, ground-laboratory ECR-exposed, and the space flight sample) were mounted using the same type and thickness sample holder for hardness characterization.

3. In-Space Exposed DC 93-500

The in-space exposed DC 93-500 sample was exposed to LEO AO as part of the EOIM III shuttle flight experiment flown on STS-46. This sample was exposed to directed ram AO from within the shuttle bay and received a LEO atomic oxygen fluence of $2.3 \pm 0.3 \times 10^{20}$ atoms/cm^2 (Ref. 3). The flight sample was 1 in. (2.54 cm) in diameter and was approximately 0.020–0.025 in. (0.051–0.064 cm) thick. The silicone received enough AO while in LEO to cause significant microcrazing of the surface. Pre- and postflight micrographs of the flight sample surface are shown in Fig. 1. A pristine control sample fabricated at the same time as the flight sample was also available for testing.

B. ECR Source AO Exposure

The ground-laboratory test samples were exposed to AO in an ECR source facility at the Lockheed Martin Space System Company Advanced Technology Center. This directional plasma system provides ~90% thermal AO (0.1 eV) and ~10% ionized species (15–20 eV). The effective exposed area is 6–8 in. (15.2–20.3-cm) diameter with ~20% drop-off at 4 in. (10.2 cm) off center. The Kapton effective atomic oxygen flux is $\sim 6 \times 10^{15}$ atoms/cm^2 s, based on mass loss measurements. Five DC 93-500 samples were exposed to ECR AO from 18 to 40 h. The sample temperature during ECR exposure was 80°C. The ground-laboratory exposed samples and the corresponding Kapton mass loss effective fluence values are provided in Table 1.

Table 1 ECR AO exposed samples

AO, h	AO Kapton effective fluence, $\times 10^{20}$ atoms/cm^2
0	0
18	4.2
20	4.7
24	5.6
30	7.0
40	9.4

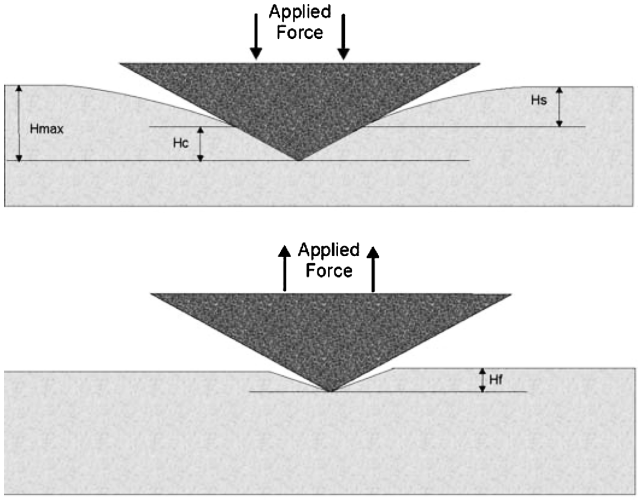

Fig. 2 Indentation profile during nanomechanical indenting.[6]

C. Nanomechanical Hardness Testing

1. Nanoindentation Background Introduction

The hardness of a material can be defined as the resistance to penetration,[4] or the resistance to plastic deformation, and is dependent on the type of test used to determine its value. Traditional hardness testers force an indenter with known geometry into the surface of a material with known applied load. Depending on the type of test, the hardness (H) is expressed by a number that is either inversely proportional to the depth of indentation for a specified load and indenter, or equal to the load (P) over the area of indentation (A), $H = P/A$ (Ref. 5). It should be kept in mind that the hardness value obtained in a particular test serves only as a comparison between materials or treatments.[5]

Nanoindentation arose from the realization that an indentation test with a sharp indenter applied with a low force is an excellent way to measure very small volumes of materials and thin films. But a need existed to be able to determine the indentation area without a high-magnification microscope. Therefore, depth-sensing indentation (DSI) techniques were developed. Nanoindentation refers to depth-sensing indentation testing in the submicrometer range. In nanoindentation techniques, the load and displacement of the indenter are recorded during the indentation process and these data are analyzed to obtain the contact area, and thereby mechanical properties, without having to see the indentations. DSI techniques provide a means for studying elastic and time-dependent plastic properties of materials.

An illustration of the mechanics of an indent along with the resulting contact depth h_c, maximum depth $h_{\max}$, and residual depth h_f is illustrated in Fig. 2 (Ref. 6). A typical nanoindentation load-displacement curve and relevant parameters used to determine mechanical properties, such as hardness and elastic modulus, are provided in Fig. 3.

In the TriboScope® system, the procedure used to calculate the hardness (H) from the load–displacement data is presented by Oliver and Pharr in Ref. 7 and is known as the Oliver and Pharr method. This method accounts for the curvature in the unloading data (nonlinear unloading) and uses a procedure for determining contact area (A) at peak load based on the indenter shape and depth of penetration. The hardness is defined as the mean pressure the

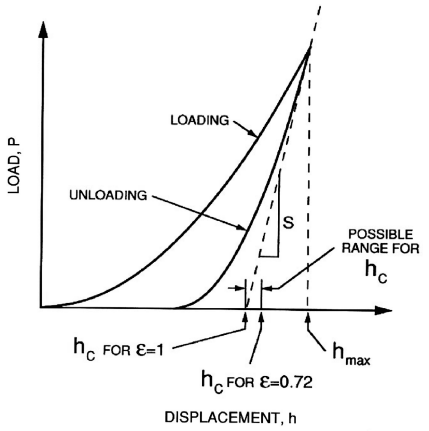

Fig. 3 Typical indentation load–displacement curve with the relevant Oliver and Pharr model parameters illustrated.[7]

material will support under load and is computed from the peak indentation load ($P_{\max}$) and the projected area of contact at peak load, $H = P_{\max}/A$ (Ref. 7).

In this method, $A = F(h_c)$. The tip area function needs to be empirically determined for each tip by performing indents into a material of known modulus to relate the cross-sectional area of the indenter to the distance from its tip.[7]

The contact depth is determined from

$$h_c = h_{\max} - \varepsilon(P_{\max}/S) \tag{1}$$

where $h_{\max}$ is the maximum loading displacement, ε is a tip geometry factor ($\varepsilon = 0.75$ for this analysis), and S is the gradient of the initial unloading curve, called the contact stiffness at unloading ($S = \mathrm{d}P/\mathrm{d}h$). This procedure is reliant on the accuracy of some key quantities including the unloading stiffness, the load frame compliance of the instrument (machine compliance), and the area function of the indenter tip.[7] It should be noted that this definition of the hardness is different from the conventional definition of hardness. In the nanoindentation analysis the hardness is calculated utilizing the contact area at maximum load, whereas in conventional tests the area of the residual indent after unloading is used; therefore the values differ.

2. *TriboScope Nanomechanical Test System*

A Hysitron, Inc., TriboScope nanomechanical test system operated in conjunction with a Park Scientific AutoProbe atomic force microscope (AFM) was used to determine the surface hardness of the silicone samples. The TriboScope nanomechanical test instrument is a quantitative depth-sensing nanoindentation system that uses a three-plate capacitive force/displacement transducer. The Hysitron nanomechanical system can provide ultralight load indentations (less than 25 μN) and continuously measures force and displacement as an indent is made. The maximum force experienced by these samples (the sample force, F_{sample}) is not the same as the prescribed applied force (the force applied to the center plate of the transducer, F_{applied}), primarily due to the large displacement of these samples with soft bulk thickness.

3. *Preliminary Nanomechanical Calibration and Testing*

Before data acquisition, a significant amount of preliminary calibration and optimization testing is necessary with a nanomechanical test system. Load-frame compliance calibration of the system (machine compliance) is necessary, using the specific type of sample holder the test samples are mounted on. Also, tip-shape area function determination needs to be conducted for the particular indenter tip used.

QSM vs DSM. The Hysitron system used for this study has both quasi-static measurement (QSM) and continuous stiffness measurement, called dynamic stiffness measurement (DSM), also referred to as nanoDMA (dynamic mechanical analysis) techniques. By taking

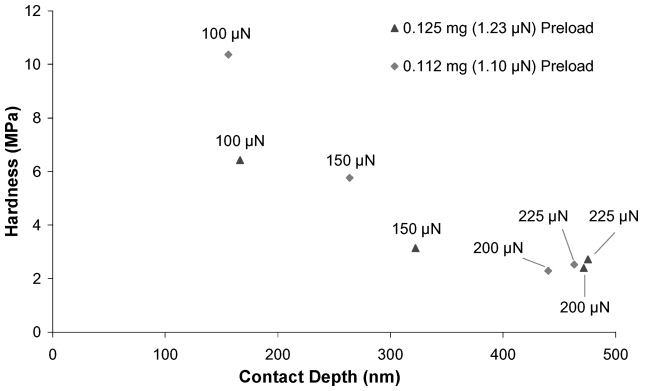

Fig. 4 Effect of preload on the hardness of the 24-h AO-exposed DC 93-500 sample for low applied indentation forces.

a series of indents at various applied indent forces using QSM and its software, a plot of the sample hardness vs contact depth can be obtained. This technique is much more time-consuming than using DSM, which can provide modulus vs depth in a single indent but does not provide hardness values. The DSM technique would be beneficial for tacky silicones, because data vs depth can be acquired in a single indent and the chance of tip contamination or breaking is greater with tacky materials. The QSM software used (TriboScope V4.1) has the ability to correct for large displacements (automatic correction of the electrostatic force constant at large displacements), which was determined to be necessary for these extremely soft samples. It was decided to use the QSM mode for data acquisition for this research because it provides hardness values in additional to modulus data for a given displacement depth.

Preload and applied indent force determination. Tests were conducted to determine the effect of the transducer tip preload and indent force on the hardness values. It is necessary to have some limited preload prior to indenting to keep the transducer tip in contact with the sample as controlled through the AFM feedback system. A preload below 0.089 mg (equivalent to 0.87-μN applied force) provided unstable tip/sample control. Indentations were made (in the 24-h AO-exposed DC 93-500 sample) at 100-, 150-, 200-, and 225-μN applied indent forces with preloads of 0.112 mg (1.10 μN), and then 0.125 mg (1.23 μN). Figure 4 indicates that the preload will significantly affect the hardness value when less than 200-μN applied indented force is used. It was determined to use a 0.112-mg preload (1.10 μN) for all applied forces of 200 μN and below.

Hold time determination for creep. Viscoelastic creep during unloading can be a problem for polymers. Therefore creep tests were conducted where different hold times (5, 10, and 20 s) were used during a trapezoid-type loading cycle. Although these tests did not indicate additional creep for the longer hold times (one would want to increase the hold time just long enough to be sure creeping had stopped prior to unloading), the curve fits for the longer hold times appeared to fit better and hence were used for all sample indent tests.

Curve fit effect. The curve fit of the sample force-vs-displacement data was found to be critical for the resulting hardness value. Including too much of the curve often resulted in a good fit too far from the initial unloading point, where the hardness data should be obtained. Therefore, for each sample indent, the best curve fit was carefully determined. An example of a sample force-vs-displacement curve for an applied force of 700 μN with a typically used fit (upper fit of 99% (includes 99% of the upper curve) and lower fit of 65% (65% of the lower curve) is shown in Fig. 5.

4. *Indentation Procedures*

The transducer tip was brought into contact with the surface of the sample using the AFM electronics and feedback system. Once in contact with the surface, the tip was left at an ultralight preload and the system was left to settle for 2 min before starting the indent, to minimize drift. Indentations in the test samples were taken using

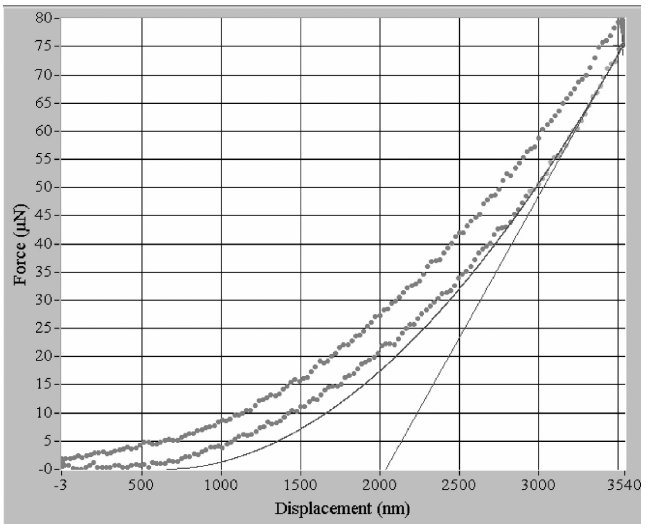

Fig. 5 Sample force vs displacement for pristine DC 93-500 with an upper fit of 99% and lower fit of 65%.

a trapezoid loading curve with a 20-s hold period (5-s ramp up, 20-s hold, 5-s ramp down) using a Berkovich indenter. A Berkovich tip is a three-sided pyramid tip with an area-to-depth function that is the same as that of a Vickers indenter.[7] The total included angle of a Berkovich tip is 142.3 deg with a half-angle of 65.35 deg. This tip geometry has been used as the standard for nanoindentation. The average radius of curvature is typically between 100 and 200 nm. Indents were made with applied forces ranging from 75 to 900 μN, and up to 1500 μN when possible. The maximum applied load was determined by the limit of the transducer displacement for each sample ($\approx$4700 nm). Each indentation was taken at a new sample location. Approximately 20–25 individual indentations were obtained for each sample. Preloads of 0.112 mg (1.10 μN) were used for less than 200-μN applied indent force indents. Preloads of 0.125 mg (1.23 μN) were typically used for higher than 200 μN load forces. In some of the earlier test sets, preloads of 0.111 mg (1.09 μN) were used for higher forces but were determined not to affect the hardness values for the higher loads.

III. Results and Discussion

A. Pristine DC 93-500 (ECR Control)

During indent testing of the pristine DC 93-500, negative unloading force values were observed in the real-time force vs displacement data during the second set of indents, possibly indicating tip contamination. Tests were conducted that verified that the sample tip was contaminated from the silicone (i.e., repeated indents were consistently "softer" than the original data taken at the same location prior to tip contamination). After tip cleaning, additional data was taken to verify that the tip was not changed. The results of the noncontaminated pristine data obtained during two separate indent sessions at two different locations are provided in Fig. 6 along with a curve fit for the data. An image of the sample surface is also provided in Fig. 6. As can be seen, the hardness of the pristine silicone is greater at the near surface than deeper in the bulk of the material. This is commonly found for both metal and polymer materials using nanoindentation techniques. Polymers typically display greater hardness values at the surface due to air- or light-induced cross linking and ambient oxidation of the surface.

B. Eighteen-Hour AO Exposed DC 93-500

The 18-h ECR-exposed sample received a Kapton effective fluence of 4.2×10^{20} atoms/cm^2. Hardness data were acquired on the 18-h AO-exposed sample during two indentation sessions at different locations. The hardness vs contact depth data are provided in Fig. 7 along with a curve fit for the data. An image of the sample surface is also provided in Fig. 7 and shows that very fine microcracks have developed.

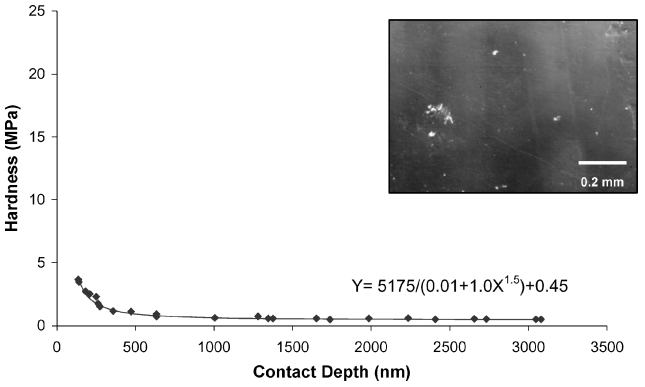

Fig. 6 Hardness vs contact depth for the pristine DC 93-500 ECR control sample.

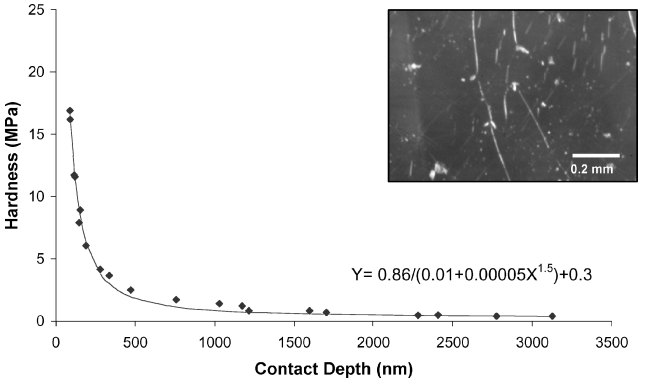

Fig. 7 Hardness vs contact depth for the 18-h ECR AO-exposed DC 93-500.

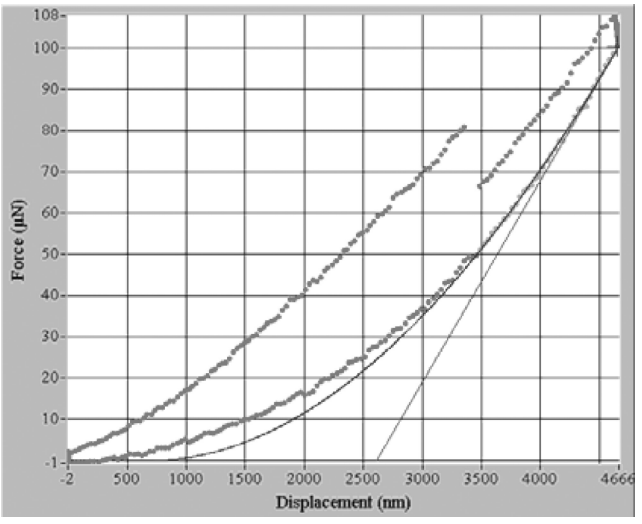

Fig. 8 TriboScope software sample force vs displacement curve for 900-μN applied force indent in the 18-h AO-exposed DC 93-500 sample.

An interesting effect was observed in the 18-h sample data at higher applied indent forces (400, 600, 800, and 900 μN). An apparent film breakthrough was displayed in the loading curve. It appears that the tip broke through a hardened surface layer and down into a softer underlying layer. An example is provided in Fig. 8 for the 900-μN applied force indent in the 18-h AO exposed sample. This type of breakthrough was observed for most of the oxidized films after some loading force is applied. It should be noted that the screen image shown in Fig. 8 provides the displacement at breakthrough, not the actual contact depth.

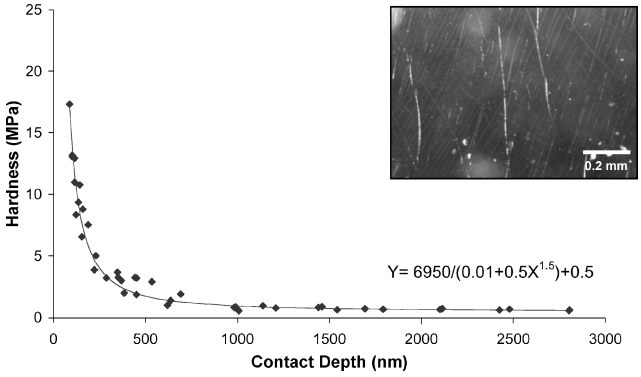

Fig. 9 Hardness vs contact depth for the 20-h ECR AO-exposed DC 93-500.

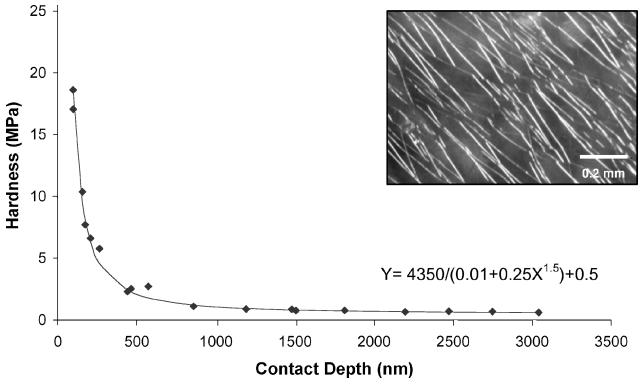

Fig. 10 Hardness vs contact depth for the 24-h ECR AO-exposed DC 93-500.

C. Twenty-Hour AO Exposed DC 93-500

The 20-h ECR-exposed sample received a Kapton effective fluence of 4.7×10^{20} atoms/cm^2. Hardness data were acquired on the 20-h AO-exposed sample during two separate indentation sessions at two different locations. The hardness vs contact depth data are provided in Fig. 9 along with a curve fit for the data. There was a fair amount of scatter in the data for contact depths between approximately 200 and 500 nm. Film breakthrough was observed when the 500-, 700-, and 800-μN applied indent forces were used. An image of the sample surface is also provided in Fig. 9 and shows that the surface has more craze lines (additional fine lines) than the 18-h exposed sample.

D. Twenty-Four-Hour AO Exposed DC 93-500

The 24-h ECR-exposed sample received a Kapton effective fluence of 5.6×10^{20} atoms/cm^2. The 24-h sample was indented during one session at two different regions. The hardness vs contact depth data are provided in Fig. 10 along with a curve fit for the data. Film breakthrough was observed for all indents at or above 200-μN applied indent forces. An image of the sample surface is also provided in Fig. 10 and shows that the surface has a well-developed crazed texture.

E. Thirty-Hour AO Exposed DC 93-500

The 30-h ECR-exposed sample received a Kapton effective fluence of 7.0×10^{20} atoms/cm^2. The hardness vs contact depth data are provided in Fig. 11, along with a curve fit for the data. Film breakthrough was observed for all indents at or above 300-μN applied indent forces. An image of the sample surface is also provided in Fig. 11 and shows that the surface has a well-developed crazed texture like the 24-h exposed sample.

F. Forty-Hour AO Exposed DC 93-500

The 40-h ECR-exposed sample received a Kapton effective fluence of 9.4×10^{20} atoms/cm^2. The hardness vs contact depth data were obtained at two separate regions of the sample. The hardness vs contact depth data are provided in Fig. 12 along with a curve fit for the data. Film breakthrough was observed for indents at or above 625-μN applied indent forces. An image of the sample surface is also provided in Fig. 12 and, like the 24- and 30-h exposed samples, shows a well-developed crazed texture.

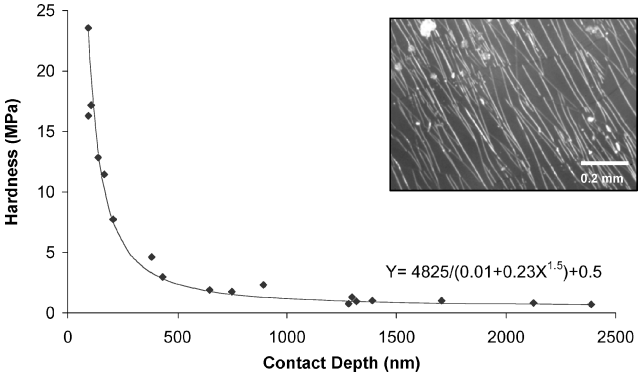

Fig. 11 Hardness vs contact depth for the 30-h ECR AO-exposed DC 93-500.

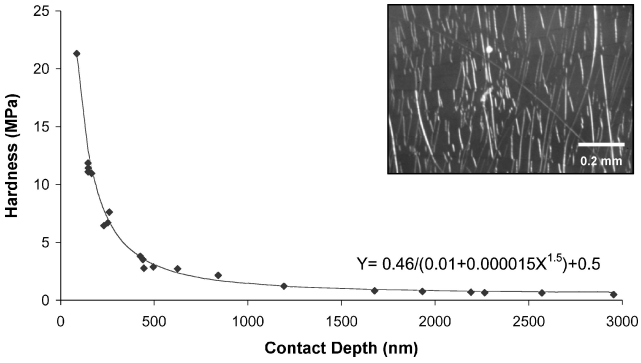

Fig. 12 Hardness vs contact depth for the 40-h ECR AO-exposed DC 93-500.

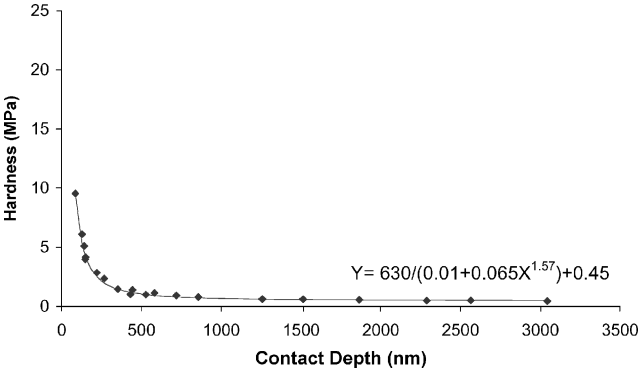

Fig. 13 Hardness vs contact depth for the EOIM III control sample fabricated at the same time as the flight sample.

G. EOIM III Control DC 93-500

The hardness vs contact depth data for the EOIM III control sample are provided in Fig. 13 along with a curve fit for the data. The surface of the control was very smooth.

H. EOIM III DC 93-500 Flight Sample

The EOIM III flight sample was exposed to a LEO AO fluence of 2.3×10^{20} atoms/cm^2. The hardness vs contact depth data are provided in Fig. 14 along with a curve fit for the data. Film breakthrough was observed for indents at 600- and 700-μN applied indent forces. An image of the sample surface is also provided in Fig. 14 and shows that the surface has a well-developed crazed texture.

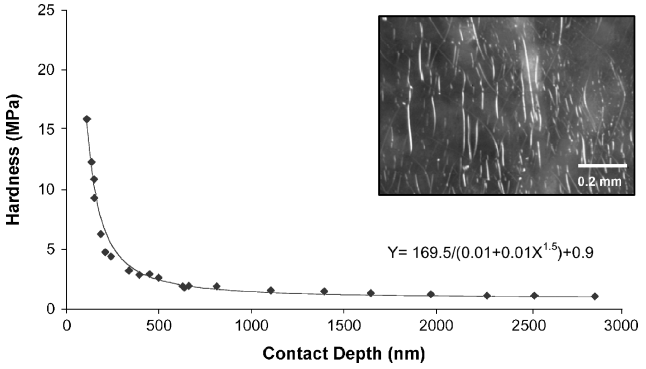

Fig. 14 Hardness vs contact depth for the EOIM III flight sample.

I. Ground-Laboratory to In-Space Effective Fluence for the ECR Facility

The AO exposure does cause surface hardening, as expected, as the silicone is oxidized. The nanomechanical hardness data indicate that the AO-exposed samples are substantially harder at the near surface than the pristine silicone. Another observation is that the hardened layer decreases with depth, as one would expect, with the hardness of the AO-exposed samples becoming the same as pristine DC 93-500 at a depth of approximately 1500 nm. The consistency of the hardness for all samples below this depth was excellent and shows excellent repeatability of this nanomechanical technique. There was a fair amount of scatter and data overlap for some samples at the low applied indent forces. Surface roughness, such as that which occurs with the "mud-tile" cracking of the oxidized silicate layer, and inhomogeneities in the surface oxide could contribute to hardness variations, particular for low-force indents.

Although film breakthrough was observed at various applied loads for all oxidized films (e.g., the ECR and flight samples), specific trends were not investigated. This would require additional analyses of the force vs distance curves to determine the specific depth of contact and applied load for which breakthrough occurred. This information was not readily available but could be obtained by analyzing the Hysitron indent data files. As previously mentioned, the observation of film breakthrough confirms that an embrittled oxidized layer has developed over the soft underlying silicone layer.

Using values obtained from the curve fit equations for each data set (the curve fit equations are given in the hardness vs depth charts); plots of hardness vs Kapton effective fluence at contact depths of 150, 200, 250, and 300 nm were produced. These depths represent the near-surface data. The 150-nm contact depth and 300-nm contact depth plots are provided in Figs. 15a and 15b, respectively. The hardness for the ECR pristine sample and the EOIM III control samples were very similar. The EOIM III control was slightly harder at a contact depth of 150 nm, which is not surprising. Even if the mix ratios and degrees of cure were the same for both controls, the EOIM III control was made years earlier; thus there would be a difference in the quantity of residual outgassing products and oxidation that could increase the hardness slightly over time. These aging differences may also affect the flight sample hardness, but are considered negligible, as the hardness difference of the two controls was determined to be insignificant at a contact depth of 150 nm (and they were essentially the same at 300 nm).

Based on the linear fits for the hardness vs Kapton effective AO fluence data, the ECR Kapton effective fluence that provided the same hardness as the EOIM III sample for 150-, 200-, 250-, and 300-nm depth was 6.10, 6.00, 6.04, and 6.16×10^{20} atoms/cm^2, respectively. Averaging these values provides 6.08×10^{20} atoms/cm^2; therefore the Kapton effective atomic oxygen fluence in the ECR facility needs to be 2.64 times higher than that in LEO to replicate equivalent exposure damage in the ground test silicone as occurred in the space exposed silicone.

When the surface crazing is compared, the extent of crazing in the 18- and 20-h ECR exposed samples appears to be less developed than that in the flight sample, while the 24-h ECR-exposed sample seems more substantially crazed like the flight sample. This is a qualitative assessment only, and may be contributed to by sample handling procedures. For comparison purposes, the hardness vs contact depth curves for the EOIM III flight sample and the 24-h ECR sample, which was closest to the necessary ECR fluence for equivalent damage, were overlaid on the pristine ECR sample data and are provided in Fig. 16.

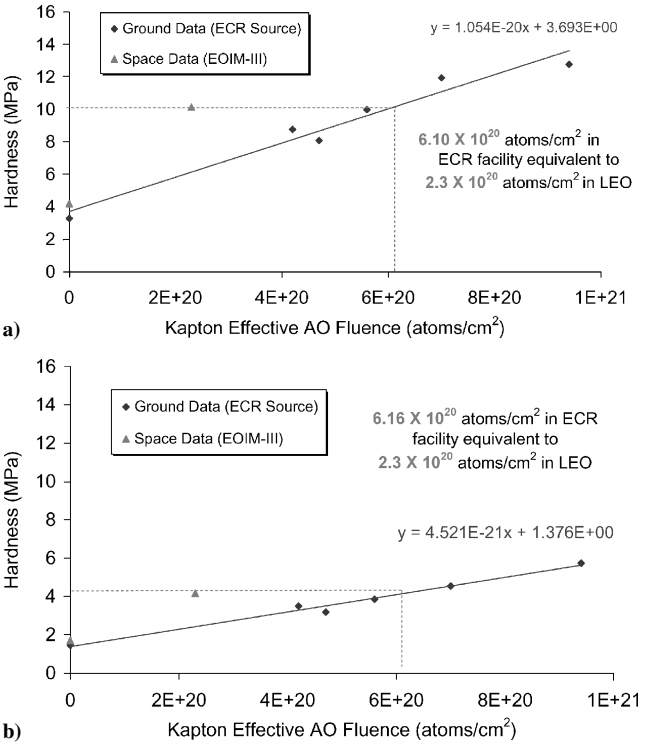

Fig. 15 Hardness vs Kapton effective AO fluence a) at contact depth 150 nm and b) at contact depth 300 nm.

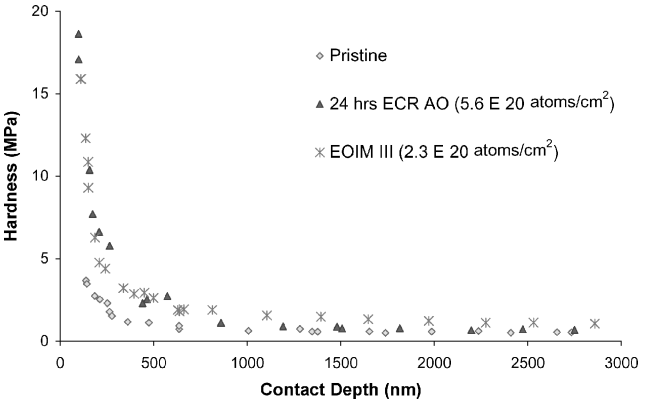

Fig. 16 Hardness vs contact depth for pristine, 24-h ECR-exposed and LEO space-exposed DC 93-500 silicone.

IV. International Space Station Application

The relevance of this method is further enhanced by correlating these results with silicone pressure-sensitive adhesive (PSA) samples that were ECR-exposed for the International Space Station solar array diode tape blocking assessment. The DC 93-500 samples as described herein were ECR-exposed simultaneously with silicone PSA samples. On-orbit, the silicone PSA surface will eventually convert to a hardened silicate glass layer, converting a sticky surface to a glassy nonblock surface. By using the correlation of ground and space DC 93-500 data, the ground-test effective fluence of the silicone PSA can be deduced and the degree of blocking vs AO

exposure that can be expected in-orbit for the diode tape can be more accurately determined.

V. Conclusions

Traditional techniques for determining effective AO fluence exposures in ground-laboratory facilities based on mass loss measurements should not be used for silicones. Therefore, a technique has been developed for ground-laboratory to in-space effective AO fluence determination for silicones based on changes in surface hardness, which occurs as the silicone is oxidized. Specifically, nanoindentation hardness measurements were determined for ground test (ECR)-exposed DC 93-500 silicone and DC 93-500 exposed to LEO AO as part of the EOIM III shuttle flight experiment. The ground-to-space effective AO fluence was determined based on the Kapton effective fluence in the ECR source that produced the same hardness for the fluence in space. Preliminary calibration and optimization testing of the nanomechanical system with silicone samples were conducted and critical issues reviewed. Hardness vs contact depth measurements were obtained for five ECR-exposed DC 93-500 samples (ECR-exposed for 18–40 h, corresponding to Kapton mass loss effective fluences of 4.2×10^{20} to 9.4×10^{20} atoms/cm^2, respectively) and for the EOIM III LEO-exposed DC 93-500 silicone. Pristine controls for the ECR tests and for the EOIM III flight sample were also measured. The ground-to-space correlation value was determined based on correlation values for four contact depths (150, 200, 250, and 300 nm), which represent the "near-surface" depth data. The results indicate that the Kapton effective AO fluence in the ECR facility needs to be 2.64 times higher than in LEO to replicate exposure damage in the ground-test silicone equivalent to that which occurred in the space exposed silicone.

Acknowledgments

The authors thank Phil Abel of NASA Glenn Research Center for his consistent help with hardware setup and introductions to the Park Scientific AFM and Hysitron systems. They also greatly appreciate all of the many helpful insights and advice on calibration and testing procedures received from Lance Kuhn and Richard Nay of Hysitron.

References

[1]Hung, C., and Cantrell, G., "Reaction and Protection of Electrical Wire Insulators in Atomic-Oxygen Environments," NASA TM 106767, Nov. 1994.

[2]American Society for Testing and Materials, "Standard Practices for Ground Laboratory Atomic Oxygen Interaction Evaluation of Materials for Space Applications," ASTM E 2089-00, West Conshohocken, PA, June 2000.

[3]Koontz, S. L., Leger, L. J., Rickman, S. L., Hakes, C. L., Bui, D. T., Hunton, D. E., and Cross, J. B., "Oxygen Interactions with Materials III—Mission and Induced Environments," *Journal of Spacecraft and Rockets*, Vol. 32, No. 3, 1995, pp. 475–482.

[4]Smallman, R. E., *Modern Physical Metallurgy*, Butterworths, Kent, England, U.K., 1985, Chap. 2.7.

[5]Avner, S. H., *Introduction to Physical Metallurgy*, 2nd ed., McGraw–Hill, New York, 1974, Chap. 1.24.

[6]Kuhn, L., "Data Analysis with the TriboScope® and TriboIndenter® Nanomechanical Testing Systems," Hysitron, Inc., Internal Memo NRL-S-003, Ver. 2.0, July 2003.

[7]Oliver, W. C., and Pharr, G. M., "An Improved Technique for Determining Hardness and Elastic Modulus Using Load and Displacement Sensing Indentation Experiments," *Journal of Materials Research*, Vol. 7, No. 6, 1992, pp. 1564–1583.

D. Edwards
Associate Editor